



Evidence of eutectic crystallization and transient nucleation in Al₈₉La₆Ni₅ amorphous alloy

Zhuang, Yanxin; Jiang, Jianzhong; Lin, Z. G.; Mezouar, M.; Crichton, W.; Inoue, A.

Published in:
Applied Physics Letters

Link to article, DOI:
[10.1063/1.1389506](https://doi.org/10.1063/1.1389506)

Publication date:
2001

Document Version
Publisher's PDF, also known as Version of record

[Link back to DTU Orbit](#)

Citation (APA):
Zhuang, Y., Jiang, J., Lin, Z. G., Mezouar, M., Crichton, W., & Inoue, A. (2001). Evidence of eutectic crystallization and transient nucleation in Al₈₉La₆Ni₅ amorphous alloy. *Applied Physics Letters*, 79(6), 743-745. <https://doi.org/10.1063/1.1389506>

General rights

Copyright and moral rights for the publications made accessible in the public portal are retained by the authors and/or other copyright owners and it is a condition of accessing publications that users recognise and abide by the legal requirements associated with these rights.

- Users may download and print one copy of any publication from the public portal for the purpose of private study or research.
- You may not further distribute the material or use it for any profit-making activity or commercial gain
- You may freely distribute the URL identifying the publication in the public portal

If you believe that this document breaches copyright please contact us providing details, and we will remove access to the work immediately and investigate your claim.

Evidence of eutectic crystallization and transient nucleation in $\text{Al}_{89}\text{La}_6\text{Ni}_5$ amorphous alloy

Y. X. Zhuang, J. Z. Jiang,^{a)} and Z. G. Lin

Department of Physics, Building 307, Technical University of Denmark, DK-2800 Lyngby, Denmark

M. Mezouar and W. Crichton

European Synchrotron Radiation Facility (ESRF), BP 220, 38000 Grenoble, France

A. Inoue

Institute of Materials Research, Tohoku University, Sendai 980-77, Japan

(Received 21 August 2000; accepted for publication 1 June 2001)

The phase evolution with the temperature and time in the process of crystallization of $\text{Al}_{89}\text{La}_6\text{Ni}_5$ amorphous alloy has been investigated by *in situ* high-temperature and high-pressure x-ray powder diffraction using synchrotron radiation. Two crystalline phases, fcc-Al and a metastable bcc- $(\text{AlNi})_{11}\text{La}_3$ -like phase, were identified after the first crystallization reaction, revealing a eutectic reaction instead of a primary reaction suggested in the literature. Time-dependent nucleation in the amorphous alloy is detected and the experimental data can be fitted by both the Zeldovich's and Kashchiev's transient nucleation models with transient nucleation times of 220 and 120 min, respectively. © 2001 American Institute of Physics. [DOI: 10.1063/1.1389506]

Al-based amorphous alloys with an Al concentration of about 90 at % have attracted much attention due to their mechanical properties, especially the high strength combined with a good ductility which is much superior to that of conventional high-strength aluminum alloys.^{1,2} The mechanical properties of partially crystallized amorphous alloys with nanometer-sized Al crystals could be even enhanced.^{3–5} These excellent mechanical properties make this family of Al-based amorphous alloys promising candidates as advanced engineering materials. The precipitation of face-centered-cubic (fcc)-Al nanocrystals from the amorphous alloys is generally assumed to be a primary reaction with long-range atomic diffusion, while Chen *et al.*⁶ suggested that the local atomic rearrangement instead of the long-range atomic diffusion is responsible for the formation of Al nanocrystals during deformation. Ye and Lu⁷ reported the formation of single fcc-Al phase after the first primary crystallization in an $\text{Al}_{89}\text{La}_6\text{Ni}_5$ amorphous alloy. On the other hand, Gogebakan *et al.*⁸ observed that the crystalline phases after the first crystallization reaction in an $\text{Al}_{85}\text{Y}_{11}\text{Ni}_4$ alloy are fcc-Al, Al_3Y , and some unidentified metastable intermetallic phases, indicating a eutectic reaction. Gangopadhyay and Kelton⁹ further investigated the crystallization processes and found that the crystallization products depend on the radius of rare-earth atoms. The x-ray powder diffraction pattern (XRD) recorded after the first crystallization reaction in an $\text{Al}_{88}\text{La}_8\text{Ni}_4$ alloy shows two crystalline phases, although the authors did not clarify the point in their work.⁹ In this work, we present experimental evidence of the eutectic crystallization reaction and transient nucleation in the $\text{Al}_{89}\text{La}_6\text{Ni}_5$ amorphous alloy by means of *in situ* high-temperature (293–673 K) and high-pressure (0–4 GPa) angle-dispersive XRD measurements using synchrotron radiation. Two crystalline phases, fcc-Al and

a metastable body-centered-cubic (bcc)- $(\text{AlNi})_{11}\text{La}_3$ -like phase, were identified after the first crystallization reaction. Time-dependent nucleation is observed in the amorphous alloy during the crystallization kinetic process and successfully described by classic transient nucleation theory.

Ingots, with nominal composition $\text{Al}_{89}\text{La}_6\text{Ni}_5$, were prepared by arc melting a mixture of pure Al (99.99 wt %), La, (99.9 wt %), and Ni (above 99.96 wt %) in a purified argon atmosphere. Details of sample preparation and characterization were reported in Ref. 10. Differential scanning calorimetry (DSC) measurements were performed in a flowing purified argon atmosphere using a Perkin-Elmer DSC-7 at a heating rate of 40 K/min. The amorphous alloy exhibits two exothermic crystallization reactions with the onset temperatures T_{x1} and T_{x2} of 494.1 K and 611.9 K, respectively. *In situ* high-pressure and high-temperature angle-dispersive XRD measurements were performed by synchrotron radiation using the Paris–Edinburgh large-volume apparatus available at European Synchrotron Radiation Facility (ESRF) in Grenoble, France with a wavelength of 0.20215 Å.¹⁰ Instrumental line broadening is negligible. The temperature was measured by means of a K-type thermocouple with a stability of ± 1 K. Each run consisted of an isothermal room-temperature compression followed by an isobaric heating to a high temperature in steps of 10 K. The average heating rate in the temperature range from 298 to 673 K was roughly estimated to be 3 K/min. The kinetic XRD patterns were recorded for each 10 min at a given temperature and pressure, in which the temperature is rapidly heated to the given one without overshoot. The pressure of the sample is calculated from the equation of state of BN.¹¹

Figure 1 exemplifies XRD patterns recorded at 2 GPa and various temperatures. A broad amorphous peak, located at $2\theta \approx 4.8^\circ$, together with Bragg peaks from BN marked in Fig. 1 and from the gasket in the 2θ range of $2\text{--}3^\circ$ are observed in the XRD patterns recorded at 298, 373, and 483 K.

^{a)} Author to whom correspondence should be addressed; electronic mail: jiang@fysik.dtu.dk

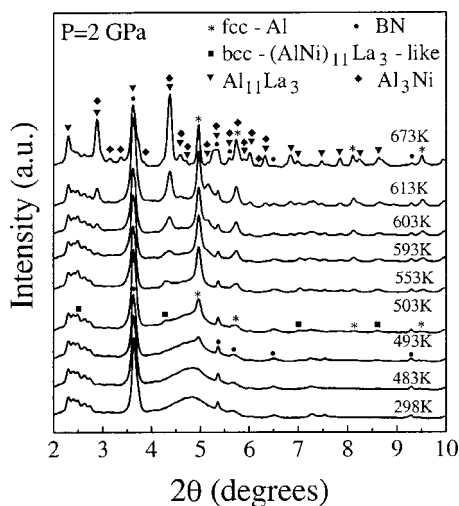


FIG. 1. *In situ* high-temperature and high-pressure XRD patterns recorded at various temperatures for the $\text{Al}_{89}\text{La}_6\text{Ni}_5$ amorphous alloy are shown.

It is seen that a new tiny crystalline peak ($2\theta \approx 5^\circ$) appears at 493 K together with four new Bragg peaks located at $2\theta \approx 2.47^\circ$, 4.26° , 6.98° , and 8.59° . The four new Bragg peaks can be indexed to a bcc structure with a lattice constant of 6.64 \AA and space group Im3m. The observed and calculated interplanar spacings of the cubic phase together with the data from Ref. 9 are listed in Table I. These Bragg peaks are very close to the corresponding peaks for the orthorhombic $\text{Al}_{11}\text{La}_3$ phase. The atomic radius of Ni is close to that of Al. Thus, it is not unreasonable to suggest that the new cubic phase could be a bcc-(AlNi) $_{11}\text{La}_3$ -like phase. This cubic phase together with the fcc-Al phase are observed in all XRD patterns recorded after the first crystallization process at various pressures. These results indicate that the first crystallization process of the $\text{Al}_{89}\text{La}_6\text{Ni}_5$ amorphous alloy is governed by a eutectic reaction rather than a primary reaction, which was suggested in the literature.⁷ With increasing temperature, the crystalline peaks become narrower in width and higher in intensity. More Bragg peaks appear in the XRD pattern recorded at 603 K, indicating that the residual amorphous phase begins to crystallize and the bcc-(AlNi) $_{11}\text{La}_3$ -like phase starts to decompose. At 673 K, fcc-Al, $\text{Al}_{11}\text{La}_3$, and Al_3Ni , together with a few tiny peaks, are detected while the bcc-(AlNi) $_{11}\text{La}_3$ -like phase disappears.

To further study the first crystallization reaction in the $\text{Al}_{89}\text{La}_6\text{Ni}_5$ amorphous alloy, *in situ* high-temperature kinetic XRD measurements were performed, as shown in Fig. 2. It is

TABLE I. Interplanar spacings of the metastable bcc-(AlNi) $_{11}\text{La}_3$ -like phase with a lattice constant of 6.64 \AA and space group Im3m obtained from the *in situ* XRD pattern recorded at 503 K and 2 GPa for the $\text{Al}_{89}\text{La}_6\text{Ni}_5$ amorphous alloy are shown. The data obtained from Ref. 9 are at ambient temperature and pressure.

hkl	$d_{\text{cal}} (\text{\AA})$	$d_{\text{exp}} (\text{\AA})$	$d_{\text{exp}} (\text{\AA})^b$
110	4.695	4.69	4.67
200	3.32 ^a		3.30
211	2.711	2.72	2.70
220	2.348 ^a		2.34
400	1.66	1.66	1.64
422	1.355	1.35	1.34

^aPeaks are overlapped with those of BN or fcc Al.

^bData are from Ref. 9.

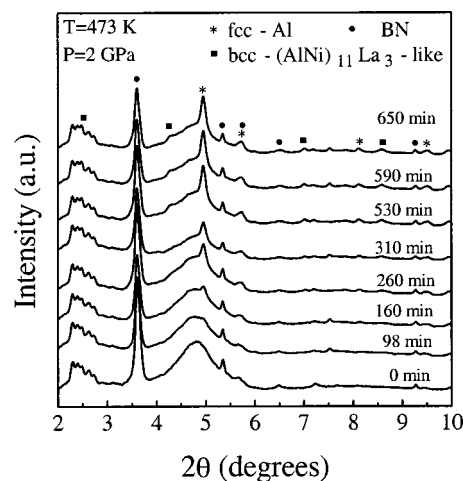


FIG. 2. *In situ* kinetic XRD patterns recorded at 473 K and 2 GPa as a function of time for the $\text{Al}_{89}\text{La}_6\text{Ni}_5$ amorphous alloy are shown.

found that the first crystalline phases formed are fcc-Al and the metastable bcc-(AlNi) $_{11}\text{La}_3$ -like phase. This result confirms that the first crystallization reaction in the $\text{Al}_{89}\text{La}_6\text{Ni}_5$ amorphous alloy is a eutectic rather than a primary reaction.

During the crystallization process, the *relative volume fraction*, f , of the crystalline component at a given time, t , is estimated from the expression: $Y(t) = (1-f)Y(0) + fY(t_{\text{max}})$, where $Y(t)$, $Y(0)$, and $Y(t_{\text{max}})$ are the XRD patterns at times of t , 0, t_{max} , respectively. t_{max} is randomly selected. Figure 3 shows the relative volume fraction as a function of time together with three theoretical fitting curves (details given later). From transmission electron microscopy measurements, it was found that during the first crystallization reaction of the amorphous alloy, the crystals rapidly grow and then saturate to a value of around 15–20 nm. It was also found in Fig. 2 that the widths of Bragg peaks remain almost constant while the instrumental line broadening is negligible. These results infer that the *relative volume fraction* might be proportional to the relative number of nucleation with a constant crystal size. Six possible nucleation and growth models were applied to fit the data in Fig. 3. They are (1) model 1: heterogeneous nucleation with constant growth rate, (2) model 2: steady-state nucleation with constant growth rate, (3) model 3: time-dependent Kashchiev's nucleation¹² with constant growth rate, (4) model 4: heterogeneous nucleation with zero growth rate (i.e., constant grain size), (5) model 5: steady-state nucleation with zero growth rate, and (6) model 6: time-dependent Kashchiev's nucleation with zero growth rate. It was found that models 3, 4, and 5 can not fit the data at all. Figure 3 shows fitting results using models 1, 2, and 6. It is clearly seen that the best fit was obtained using the model 6 with a transient time of 120 min. Due to fast nucleation processes in amorphous alloys, steady-state nucleation has been considered in most cases. Very few comprehensive experimental investigations of time-dependent nucleation in metallic glasses have been reported.^{13,14} In the classic transient nucleation theory, two analyses, based on the Zeldovich–Frenkel equation,¹⁵ were proposed. One is the Zeldovich's equation. Zeldovich¹⁵ assumed that the work of formation of a nucleus with size of n is proportional to n^2 and the rate of monomer addition to a nucleus with size of n , $k_n^+ \approx k_n^*$, and found a time-

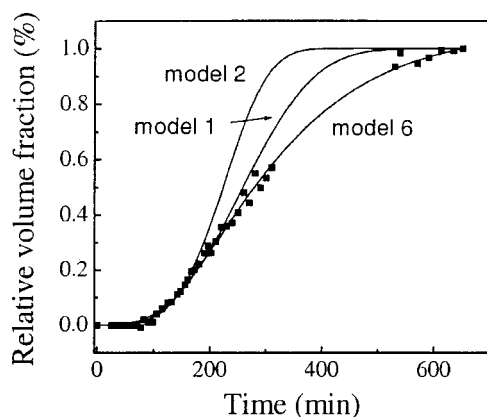


FIG. 3. Relative volume fraction of the crystalline component with time during the isothermal annealing at 473 K and 2 GPa for the $\text{Al}_{89}\text{La}_6\text{Ni}_5$ amorphous alloy, having $t_{\text{max}}=650$ min is shown. In the time period of about 310–510 min, synchrotron radiation x-ray beam was lost in the storage ring during the measurement.

dependent nucleation rate, $I_{n^*}(t)$, at the critical size n^* as:

$$I_{n^*} = I_{\text{st}} \exp(-\tau_z/t), \quad (1)$$

where τ_z is the transient nucleation time, $\tau_z = (256\pi\sigma^6 v^4)/(9\delta\mu^6 k_n^+)$, $\delta\mu$ is the difference of the Gibbs free energies per molecule between the crystalline and amorphous phases, σ is the interfacial energy per unit area, and v is the molecular volume. The other is the Kashchiev's equation.¹² Kashchiev further studied the transient nucleation process and performed the most thorough analytical treatment of the Zeldovich–Frenkel equation. Based on two assumptions: (1) the work of the formation of a nucleus with size of n is approximated by the first two nonzero terms in a Taylor expansion about n^* , and (2) $k_n^+ \approx k_{n^*}^+$, he derived the time-dependent nucleation rate as:

$$I_{n^*} = I_{\text{st}} \left[1 + 2 \sum_{m=1}^{\infty} (-1)^m \exp\left(-\frac{m^2 t}{\tau_K}\right) \right], \quad (2)$$

where τ_K is the transient nucleation time, $\tau_K = (256k_B T \sigma^3 v^2)/(\pi \delta\mu^4 k_{n^*}^+)$, k_B is the Boltzmann's constant, and T is the temperature. The ratio of the transient nucleation times in both models is given by $\tau_z/\tau_K = (\pi^3 \sigma^3 v^2)/(9k_B T \delta\mu^2)$. Both transient nucleation models can well fit the data in Fig. 3 with $\tau_z=220$ min and $\tau_K=120$ min. The induction time, θ , defined by the extrapolation of the steady-state nucleation behavior to the time axis, and the steady-state time, t_{st} , at which the nucleation rate is time independent,¹⁶ are estimated to be $\theta=116$ min and $t_{\text{st}}=160$ min, respectively, as shown in Fig. 4. The induction time, θ , is most directly related to the transient nucleation time, τ .¹⁶ It is clear that the transient nucleation time, $\tau_K=120$ min, derived from the Kashchiev's model, is much closer to the induction time, $\theta=116$ min, than $\tau_z=220$ min derived from the Zeldovich's model. For the $\text{Al}_{89}\text{La}_6\text{Ni}_5$ amorphous alloy, using $\sigma=0.108$ J/m² for the liquid–solid interfacial energy of aluminum,¹⁶ molar volume of about 10 cm³/mol for the fcc Al and $T=473$ K, the Gibbs free energy

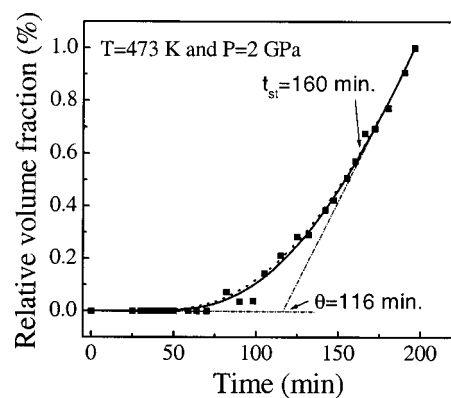


FIG. 4. Relative volume fraction of the crystalline component with time during the isothermal annealing at 473 K and 2 GPa for the $\text{Al}_{89}\text{La}_6\text{Ni}_5$ amorphous alloy, having $t_{\text{max}}=196$ min is shown. The induction time, θ , and the steady-state time, t_{st} , are estimated to be 116 min and 160 min, respectively. The solid and dashed curves are the Zeldovich's and Kashchiev's transient nucleation rate equations with $\tau_z=220$ min and $\tau_K=120$ min, respectively.

difference per molar between the crystalline and amorphous phases is estimated to be about 602 J/cm³ at 473 K and 2 GPa.

In summary, the phase evolution with the temperature and time in the crystallization processes of $\text{Al}_{89}\text{La}_6\text{Ni}_5$ amorphous alloy has been investigated by *in situ* high-temperature and high-pressure XRD using synchrotron radiation. It is found that the first crystallization process is a eutectic reaction with two crystalline phases, fcc Al and the metastable bcc-(AlNi)₁₁La₃-like phase. The experimental data, the relative volume fraction of the crystalline component as a function of time, can be described by both the Zeldovich's and Kashchiev's transient nucleation models. The Gibbs free energy difference per molar between the crystalline and amorphous phases is estimated to be about 602 J/cm³ at 473 K and 2 GPa.

¹ A. Inoue, K. Ohtera, A. P. Tsai, and T. Masumoto, Jpn. J. Appl. Phys., Part 2 **27**, L280 (1988).

² Y. He, S. J. Poon, and G. J. Shiflet, Science **241**, 1640 (1988).

³ H. Chen, Y. He, G. J. Shiflet, and S. J. Poon, Scr. Metall. Mater. **25**, 1421 (1991).

⁴ A. Inoue, Prog. Mater. Sci. **43**, 365 (1998).

⁵ T. Gloriant and A. L. Greer, Nanostruct. Mater. **10**, 389 (1998).

⁶ H. Chen, Y. He, G. J. Shiflet, and S. J. Poon, Nature (London) **367**, 541 (1994).

⁷ F. Ye and K. Lu, Acta Mater. **47**, 2449 (1999); Phys. Rev. B **60**, 7018 (1999); J. Non-Cryst. Solids **262**, 228 (2000).

⁸ M. Gogebakan, P. J. Warren, and B. Cantor, Mater. Sci. Eng., A **226**, 168 (1997).

⁹ A. K. Gangopadhyay and K. F. Kelton, Philos. Mag. A **80**, 1193 (2000).

¹⁰ Y. X. Zhuang, J. Z. Jiang, T. J. Zhou, H. Rasmussen, L. Gerward, M. Mezouar, W. Crichton, and A. Inoue, Appl. Phys. Lett. **77**, 4133 (2000).

¹¹ Y. Le Godec, D. Martinez-Garcia, M. Mezouar, G. Syfosse, J. P. Itie, and J.-M. Besson (unpublished).

¹² D. Kashchiev, Surf. Sci. **14**, 209 (1969).

¹³ S. Brauer, H. E. Fischer, J. O. Strom-Olsen, M. Sutton, A. Zaluska, and G. B. Stephenson, Phys. Rev. B **47**, 11757 (1993).

¹⁴ M. Bushwitz, R. Adlwarth-Dieball, and P. L. Ryder, Acta Metall. Mater. **41**, 1885 (1993).

¹⁵ J. B. Zeldovich, Acta Physicochim. URSS **18**, 1 (1943); J. I. Frenkel, Kinetic Theory of Liquids (Oxford University Press, London, 1946).

¹⁶ K. F. Kelton, Solid State Phys. **45**, 75 (1991).